Statistical quantification of earthquake effects on the excavation damage zone

Md Abdullah Asad, Magdalena Krol, Matthew A Perras
Civil Engineering, York University, Toronto, Ontario, Canada

ABSTRACT
Deep geological repositories are being designed to manage spent nuclear fuel of past and future reactors for up to 1 million years across the world. The geosphere surrounding a repository should be structurally stable against geological perturbations, such as earthquakes. Previous studies have evaluated earthquake effects on the repository showing that, there is a measured change in excavation damage zone due to a low probability earthquake event. However, a quantitative study has yet to be performed considering extreme events. In this study, a two-dimensional model was developed in RS2, from Rocscience, a finite element package and compared to a previous repository seismic model. The model utilized a Voronoi joint network around the repository to represent a crystalline rock formation (host rock) and allow for excavation induced damage to evolve during construction. The host rock as well as the engineered barrier system were then subjected to glacial induced stress and earthquake loading. This model was then used to perform a statistical study using analysis of variance (ANOVA) to quantify the earthquake effects. The ANOVA analysis (significance level of 0.05) examined normal and shear stresses and displacements along the Voronoi joints after earthquake events of different seismic coefficients (model coefficients used to represent the peak ground acceleration as a fraction of the acceleration due to gravity), relative to the model with no earthquake events and no glacial loading. Glacial loading caused additional damage in the repository excavation damage zone and had statistically significant effect on joint normal stress. The seismic coefficients had no statistically significant effect on the joint parameters, although only the final state after the earthquake loading was investigated. Future research will examine the dynamic loading response during an earthquake.

RÉSUMÉ
Tout autour du monde, des entrepôts géologiques profonds sont en train d'être conçus pour la gestion des déchets radioactifs et des combustibles nucléaires usés pour une durée allant jusqu'à 1 million d'années. En effet, le milieu autour de ces réservoirs d'entreposage doit être structurellement stable, pour résister les effets des perturbations géologiques telles que les tremblements de terre. Des études précédentes ont évalué ces effets, montrant qu'il y a de changements mesurés dans les zones d'excavation affectées par des séismes à faible probabilité. Cependant, une étude quantitative considérant les événements géologiques extrêmes n'a pas encore été réalisée. Dans cette étude, on adresse cette question par un modèle bidimensionnel conçu en RS2, un logiciel d'éléments finis, développé par Rocscience. Ce modèle a été comparé avec un modèle précédent pour un entrepôt en zones sismiques. Le modèle proposé utilise un réseau de Voronoi pour décrire une formation rocheuse cristalline (roche hôte) autour du repositoire et a permis d'évaluer les dommages résultants de l'excavation durant la construction. La roche hôte aussi bien que le système de barrières de protection ont été soumis aux efforts de la glaciation et des tremblements de terre. Ce modèle a été ensuite utilisé pour développer une étude statistique basée sur une analyse ANOVA de variances pour quantifier les effets de tremblements de terre. L'analyse ANOVA avec un 0.05 seuil de signification, a examiné les efforts normaux, les efforts de cisaillement et les déplacements sur les « joints » de Voroni après des tremblements de terre, en utilisant des coefficients sismiques différents. Les coefficients du modèle ont été utilisés pour représenter l'accélération maximale du sol par rapport à l'accélération gravitationnelle. Ceci a été comparé au modèle sans évènement sismique et sans effort de glaciation. On montre que les efforts de la glaciation causent des dommages additionnels dans la zone d'excavation reliée au repositoire et ont des effets significatifs sur l'ensemble des efforts normaux. On établit que les coefficients sismiques n'ont pas d'effet statistiquement significatif sur les paramètres, malgré le fait que seulement l'état final, après les efforts sismiques, a été considéré. Dans l'avenir, on compte examiner la réponse aux efforts dynamiques pendant un tremblement de terre.

1 INTRODUCTION

Many countries, including Canada, are considering deep geological repositories (DGRs) as a long-term solution for safe storage of used nuclear fuel. A DGR is a system consisting of an arrangement of the underground facility (i.e., tunnels and placement rooms) to store used fuel containers (UFCs) and other by products of operating nuclear power plants (NWMO 2019). It is an internationally accepted technique (Boyle and Meguid 2015, NWMO 2018) for long-term UFC management. The NWMO is investigating a DGR in crystalline (granite) or sedimentary rock at an approximate depth of 500 m below the ground surface (NWMO 2015). Figure 1 shows the conceptual layout of the Canadian DGR, which consists of surface facilities, main shaft complex, placement rooms, and a ventilation shaft (NWMO 2015). The surface facilities will be used to receive, inspect, repackage the UFCs in rectangular barrier boxes and move them to the main shaft complex (Noronha 2016). The main shaft complex will be used to transfer these boxes to the underground repository. Then they will be embedded in horizontal placement rooms. DGRs are designed with multiple barriers consisting of engineered and natural barriers (Figure 1). The engineered barrier system (EBS) around the UFC includes a bentonite buffer box (made up of highly compacted bentonite (HCB)), bentonite spacer block to separate the buffer boxes and dense bentonite backfill (DBF) to cover open spaces in the placement rooms. The host rock acts as a natural barrier.

The DGR should be sited in a seismically stable formation (CNSC 2018) and assessing vulnerabilities due to future earthquakes is important. Seismic hazard assessment of DGRs has been studied in some countries (Baeckblom and Munier 2002, Guzina et al. 2015, McEvoy et al. 2016, Kaláb et al. 2017). Generally, damage within the excavation damage zone (EDZ) of a DGR (i.e., Rock damage around the excavation) due to seismic loading depends on the probability of earthquake occurrence, magnitude, distance from the DGR and peak ground acceleration (PGA) (Guzina et al. 2015). This information can be obtained from the geological history of a prospective DGR site for numerical analysis. Guzina et al. (2015) studied the effect of earthquakes for a conceptual Canadian DGR in both sedimentary and crystalline rock. They considered different earthquake events likely to occur in a long-term period in the Canadian DGR and compared the damage due to the earthquake with the damage due to other geological perturbations. They opined that future earthquakes would not affect the DGR stability to a great extent. However, they did not quantify specifically the effect of earthquake events on the conceptual DGR stability. In this work, a two dimensional (2D) model in crystalline rock was developed in RS2, a finite element package and compared to the seismic model of Guzina et al. (2015). This model was then used to perform a statistical study, analysis of variance (ANOVA), to quantify the earthquake effect.

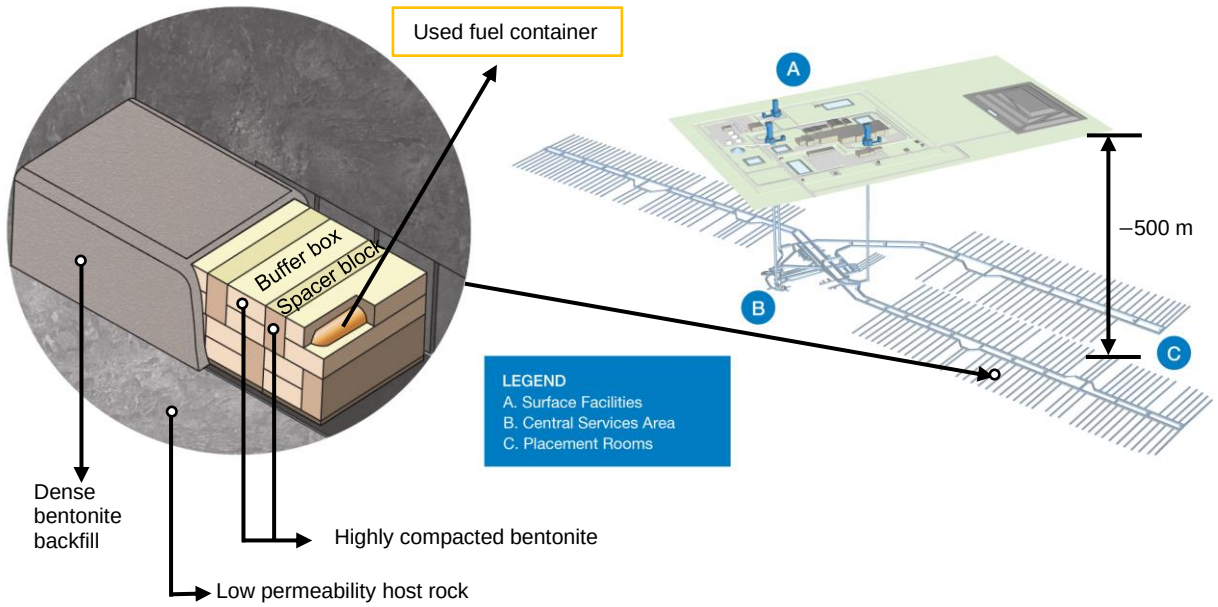

Figure 1. Conceptual multiple barrier system for the Canadian DGR (Modified from Noronha 2016), A) Surface facilities, B) Central services area and C) Placement rooms

2 MODELLING APPROACH

In this section, the modelling approach for the developed 2D model is discussed. Constitutive characteristics of rock and EBS, boundary conditions, Voronoi approximation, adjustment of Voronoi properties, simulation stages, verification and validation procedures are explained. Specifically, modelling assumptions, simplifications, required adjustments due to simplifications, qualitative comparison of results with a previous repository seismic model as one of the ways of validation are the key components of this section.

2.1 Rock mass and bentonite properties

The elastoplastic properties of granite were approximated by Voronoi network (discussed in Section 2.3) and the constitutive behaviour of HCB and DBF was set to elastic (Table 1). The in-situ stresses were calculated according to the NWMO underground repository design criteria (NWMO 2014). The maximum, minimum and vertical in situ stresses were 36.7, 25.10 and 13.5 MPa, respectively. The model was able to take horizontal and vertical PGAs.

Table 1. Granite rock mass properties (adapted from Guzina et al. (2015))

Properties	Granite	HCB	DBF
Cohesion (MPa)	14	–	–
Friction angle (°)	59	–	–
Tensile strength (MPa)	1.7	–	–
Young's modulus (GPa)	39.1	100	200
Poisson's ratio (−)	0.3	0.1	0.1
Unit weight ($MN.m^3$)	0.027	0.016	0.021

2.2 Voronoi block approximation

The granite host rock mass around the placement room was represented by Voronoi blocks. The Voronoi approximation is a numerical technique to represent the microstructure of rock through a discrete network of polygonal joint elements, which interact with their contacts. While continuum models cannot simulate the damage in the contact boundaries of rock grains or domains, the Voronoi is useful to simulate the micromechanical damage in intact rock (Sinha and Walton 2018). In addition, the brittle damage behavior of rock can be represented by Voronoi more realistically. The Voronoi contacts do not represent the actual interlock of rock grains but can help to trace and determine rock mass damage represented by contact failure in shear or tension (Guzina et al. 2015). Figure 3 shows the Voronoi network with micro properties of blocks (Youngs modulus (E^m) and Poisson ratio (ν^m)) and contacts (contact normal stiffness (k_n), contact shear stiffness (k_s), contact peak cohesion (C^m), contact peak friction ($\emptyset^m$),contact peak tensile strength (t^m)). Generally, the Voronoi block stiffness is much greater (about 10 times) than contact stiffness (Guzina et al. 2015) and failure is governed by contact stiffness. An elastoplastic behavior of the Voronoi joint elements was considered by introducing residual properties to the Voronoi joint network.

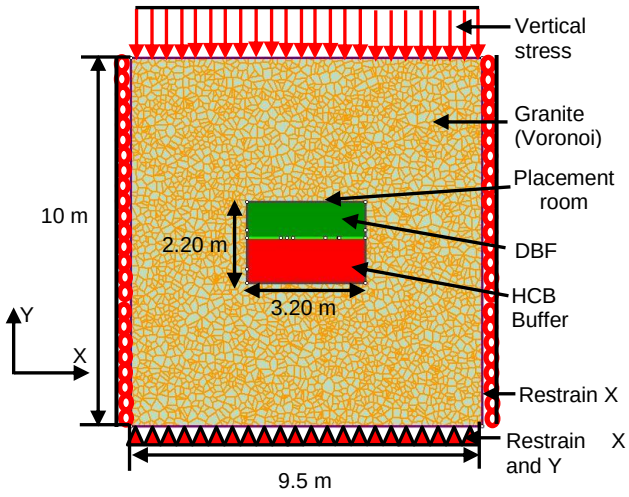

Figure 2. Boundary conditions of the RS2 model

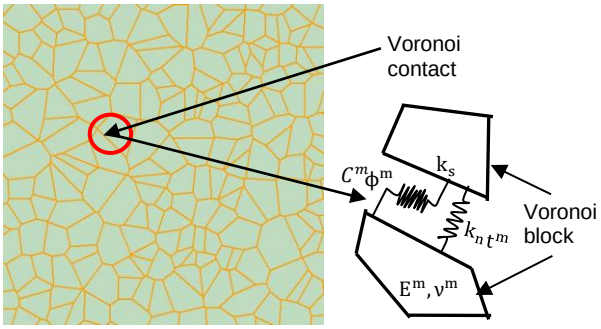

Figure 3. Voronoi contact characteristics (adapted from Guzina et al. (2015))

The micromechanical properties of the Voronoi blocks and contacts were determined by Guzina et al. (2015) by a calibration process that matched the macromechanical behavior of the intact rock estimated from laboratory experiments with the micromechanical behavior of Voronoi blocks and contacts in a numerical simulation of laboratory compression test. In this study, the calibrated micromechanical properties from Guzina et al. (2015) were adjusted. This adjustment was needed as the developed model is a simplified version of the seismic model of Guzina et al. (2015). Table 2 shows the calibrated and adjusted properties used in this study. Figure 4 shows the stages which enabled the model to consider typical DGR construction stages, buffer placement and applciation of geological perturbations. The internal pressure at the first stage was equal to the in-situ stress that reduced to zero at the placement stage. This was done to replicate the DGR construction process before placing buffer. The model was meshed with six noded triangular elements.

Table 2. Calibrated (Guzina et al. 2015) and adjusted Voronoi properties

Voronoi properties	Calibrated	Adjusted
Block Young's modulus (GPa)	588	288
Block Poisson's ratio $(-)$	0.2	0.2
Contact normal stiffness $(\mathrm{GPa.m^{-1}})$	573	173
Contact shear stiffness $(\mathrm{GPa.m^{-1}})$	287	87
Contact peak cohesion (MPa)	56.5	35
Contact peak friction $(°)$	35	22
Contact peak tensile strength (MPa)	3.63	1.63
Contact residual friction $(°)$	15	9
Contract residual cohesion (MPa)	0	0
Contact residual tensile strength (MPa)	0	0

2.3 Model validation and verification

To validate the model, damage around the placement room at stage 7 and 9 from Guzina et al. (2015) and this study were compared qualitatively (Figure 5). As seen in Figures 5a and 5b, joints are yielded at a close distance around the placement room. In Figures 5c and 5d, damage originates from the placement room corners and extends up to the corner boundaries. Therefore, the developed model showed a similar pattern of damage development between the Guzina et al. (2015) study and the model used in the present study.

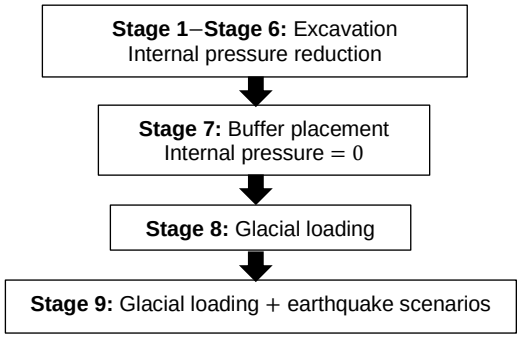

Figure 4. DGR construction and loading simulation

Verification was done by checking model results. Concentrated stresses (i.e., major and minor principal stresses) were observed around the placement room walls at stage 7 and they extended up to the boundaries at stage 9. Glacial loading caused more vertical displacement than horizontal displacement. For example, vertical displacement was 3.08×10^{-2} m and horizontal displacement was 5.25×10^{-3} m near the top boundary at stage 9 (glacial loading with a M-7.4 earthquake). Similarly, total displacement was high near the top boundary. Total displacement increased in different excavation stages (Stage 1−Stage 6) due to internal pressure reduction. Comparatively small displacements occurred at the bottom boundary as it was restrained in both directions. These verifications are in line with expected results and ensured that the model could be used for statistical analysis.

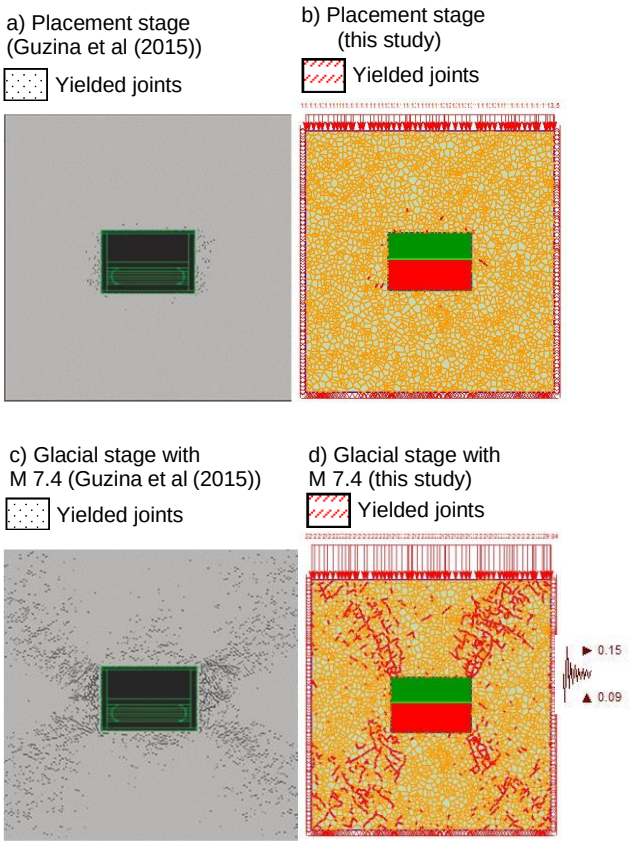

Figure 5. Comparison of damage from Guzina et al. (2015) and this study

3 STATISTICAL QUANTIFICATION PROCESS

In this section, the statistical method, ANOVA and its application to the developed model are discussed. Simulated cases for ANOVA, null hypothesis in ANOVA and application of null hypothesis are discussed. In addition, estimation of joint parameters pertinent to ANOVA is explained.

3.1 Simulated cases for sensitivity analysis

To examine the earthquake effect on the EDZ, six cases were established (Table 3). Each case had constant glacial load and different earthquake scenario except the base case 1 (Stage 7: Buffer placement), that had no glacial load or earthquake and case 2, that had no earthquake. Case 3 had an earthquake event of M-7.4, 200 km from the DGR. Case 4 had an earthquake event of M-5.25, 10 km from the DGR. These earthquake events were simulated in the seismic model of the Canadian DGR by Guzina et al. (2015). The seismic coefficients in Case 4 were greater than Case 3 as the earthquake epicenter was closer. Case 5 had an earthquake event of M-10 which is greater than any recorded earthquake in history (Hayes et al. 2020), and

was used to round up above the maximum. Case 6 used hypothetical seismic coefficients which represented a case beyond the extreme upper bound, chosen to observe the sensitivity of seismic coefficients on the EDZ.

Table 3. Simulated cases for one-factor ANOVA (Glacial loading and earthquake scenarios are taken from Guzina et al. (2015) except for case 5 - used to round up above the maximum, and case 6 - a case beyond the extreme upper bound).

Case	Glacial load (MPa)	Earthquake PGA H	V	Magnitude, distance from DGR
1	–	No earthquake		–
2	29.8	No earthquake		–
3	29.8	0.15	0.09	M-7.4, 200 km
4	29.8	0.50	0.36	M-5.25, 10 km
5	29.8	1.2	0.9	M-10, X
6	29.8	5	4.2	Y

Note: H: horizontal seismic coefficient, V: horizontal seismic coefficient. X: distance for an earthquake of maximum possible magnitude, Y: distance for case beyond the upper bound.

3.2 One-Factor analysis of variance

The one-factor ANOVA is a statistical method that calculates the effect of one factor (Montgomery and Runger 2007). The one-factor ANOVA can be represented as follows:

$$x_{ij} = \mu + \tau_i + \epsilon_{ij} \quad [1]$$

where x_{ij} is the value of a random variable at j^{th} observation under i^{th} factor, μ is the overall mean, τ_i is the factor effect and ϵ_{ij} is the random error component (Montgomery and Runger 2007). In this study, x_{ij} was the random variable which defined joint parameters (i.e., normal and shear stresses; normal and shear displacements), while the factors (τ_i) were seismic coefficients. The one-factor ANOVA assumed that the observations are done in a random order and the effect of a factor was quantified by the null hypothesis.

3.2.1 Null hypothesis

The null hypothesis (H_0) can be written as follows and states that the means are statistically equal (Montgomery and Runger 2007):

$$H_0: \mu_1 = \mu_2 \quad [2]$$

To test this hypothesis, the statistical Fisher (F) test was performed, and the results were given in terms of the P value. The Fisher test was selected since it is suitable for relatively small sample sizes (68 in this study) (Fisher 1922, 1954). To check the null hypothesis, a statistically significant level of P = 0.05 was used. In other words, if the P value > 0.05 then the null hypothesis was not rejected, and therefore the factor had no significant effect on the parameter. If the P value $\leq$ 0.05 then the null hypothesis was rejected meaning that the means being compared were statistically not equal, and thus, the factor had a statistically significant effect on the parameter.

3.3 Estimation of joint parameters

In order to assess and quantify the earthquake damage on the EDZ, four joint parameters were used. These included normal stress, shear stress, normal displacement and shear displacement. Two continuous yielded lines (dashed white line, Figure 6) consisting of 68 joints were considered for measurement. Parameter values of this yielded line were exported from RS2 to perform the one-factor ANOVA.

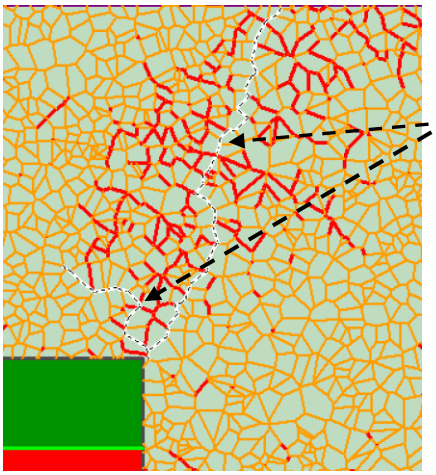

Figure 6. Parameter measurement along the dashed line through the yielded joints (red segments) region extending away from the excavation surface.

4 RESULTS AND DISCUSSIONS

The one factor ANOVA was performed by changing the seismic coefficients as outlined in Table 3. To examine the effect of seismic coefficients, various cases were simulated and a one-factor ANOVA analysis was performed to examine the effect of earthquakes on various stresses and displacements.

Table 4a. P values from one-factor ANOVA, considering C-1 as the base case

Properties	C-1:C-2:C-3 P	C-1:C-2:C-4 P	C-1:C-2:C-5 P	C-1:C-2:C-6 P
Normal stress	**2.50E-5**	**2.48E-5**	**2.44E-5**	**2.08E-5**
Shear stress	0.111	0.110	0.108	0.075
Normal displacement	0.745	0.746	0.747	0.750
Shear displacement	0.535	0.534	0.533	0.535

Table 4b. P values from one-factor ANOVA, considering C-2 as the base case

Properties	C-2:C-3 P	C-2:C-4 P	C-2:C-5 P	C-2:C-6 P
Normal stress	0.999	0.999	0.997	0.984
Shear stress	0.967	0.961	0.945	0.663
Normal displacement	0.993	0.994	0.997	0.997
Shear displacement	0.980	0.981	0.983	0.976

Note: P: P value, C-1: Case 1, C-2: Case 2, C-3: Case 3, C-4: Case 4, C-5: Case 5, C-6: Case 6. Shaded values indicate P values equal to or below 0.05; P values close to 0.05 are indicated by light green shade.

4.1 Earthquake Effect on Joint Normal Stress

Figure 7 shows the effect of glacial loading and seismic coefficients on the joint normal stress using boxplots. The median of the boxplot is represented by a central line, while the upper and lower edges of the boxplot represent the upper and lower quartiles, respectively. The tails of the distributions are represented by whiskers (dashed lines) of the boxplot. As seen in Figure 7, there was notable change in the median when adding glacial loading but very little or no change in the median for changing seismic coefficients. For all distributions, P values ranged between 2.08×10^{-5} to 2.50×10^{-5} (Table 4a) which is smaller than the significance level and therefore the null hypothesis was rejected. Further investigation was done to find out whether statistically significant impact was due to glacial loading or earthquake. For all distributions, P values ranged between 0.984 to 0.999 (Table 4b, considering case 2 as the base case) which is larger than the significance level and therefore the null hypothesis was not rejected. In other words, changes in the seismic coefficient had no statistically significant effect on the joint normal stress but glacial loading had statistically significant effect on the joint normal stress.

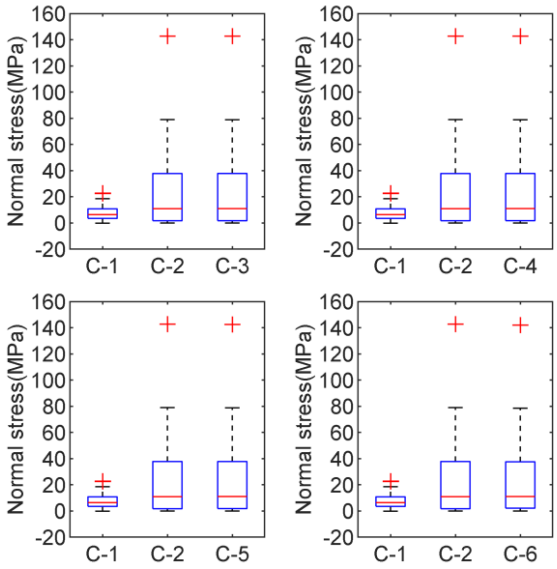

Figure 7. Effect of glacial and seismic loading on joint normal stress (C-1: Case 1, C-2: Case 2, C-3: Case 3, C-4: Case 4, C-5: Case 5, C-6: Case 6)

4.2 Earthquake Effect on Joint Shear Stress

Figure 8 shows the effect of glacial loading and seismic coefficients on the joint shear stress. As seen in Figure 8, there was notable change in the median when adding glacial loading but very little (e.g., case 6) or no change in the median for changing seismic coefficients. Case 2 and seismic cases (Case $3-6$) had noticeable outliers but they did not affect the accuracy of ANOVA as they are within the data range of case 1.

For all distributions, P values ranged between 0.075 to 0.111 (Table 4a) which is larger than the significance level and therefore the null hypothesis was not rejected. For all distributions, P values ranged between 0.663 to 0.967 (Table 4b, considering case 2 as the base case) which is larger than the significance level and therefore the null hypothesis was not rejected. In other words, glacial loading and changes in the seismic coefficient had no statistically significant effect on the joint shear stress.

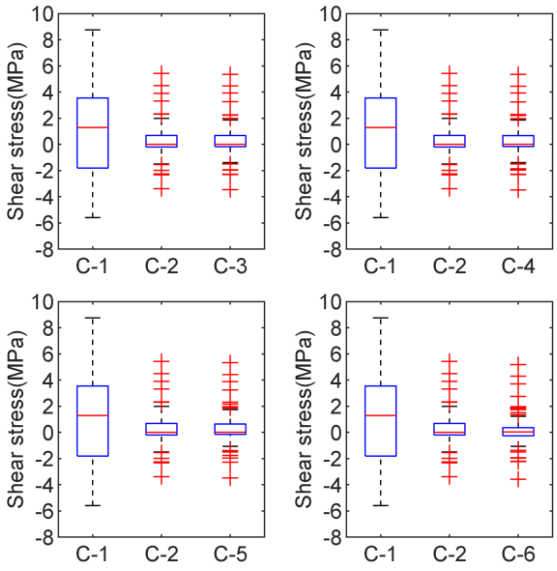

Figure 8. Effect of glacial and seismic loading on joint shear stress (C-1: Case 1, C-2: Case 2, C-3: Case 3, C-4: Case 4, C-5: Case 5, C-6: Case 6)

4.3 Earthquake Effect on Joint Normal Displacement

Figure 9 shows the effect of glacial loading and seismic coefficients on the joint normal displacement. All the box plots show very little or no change in the median value. For all distributions, P values ranged between 0.745 to 0.750 (Table 4a) which is larger than the significance level and therefore the null hypothesis was not rejected. For all distributions, P values ranged between 0.993 to 0.997

(Table 4b, considering case 2 as the base case) which is larger than the significance level and therefore the null hypothesis was not rejected. In other words, glacial loading and changes in the seismic coefficient had no statistically significant effect on the joint normal displacement.

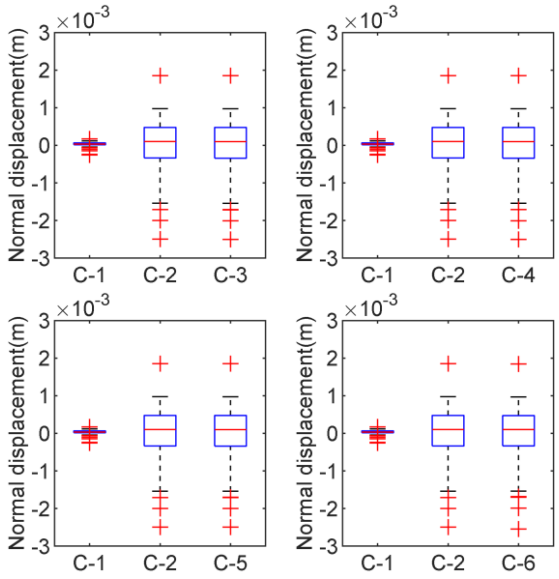

Figure 9. Effect of glacial and seismic loading on joint normal displacement (C-1: Case 1, C-2: Case 2, C-3: Case 3, C-4: Case 4, C-5: Case 5, C-6: Case 6)

4.4 Earthquake Effect on Joint Shear Displacement

Figure 10 shows the effect of glacial loading and seismic coefficients on the joint shear displacement. As seen in Figure 10, there was notable change in the median when adding glacial loading but very little or no change in the median for changing seismic coefficients.

For all distributions, P values ranged between 0.533 to 0.535 (Table 4a) which is larger than the significance level and therefore the null hypothesis was not rejected. For all distributions, P values ranged between 0.976 to 0.983 (Table 4b, considering case 2 as the base case) which is larger than the significance level and therefore the null hypothesis was not rejected. In other words, glacial loading and changes in the seismic coefficient had no statistically significant effect on the joint shear displacement. These results indicate that the DGR may not be impacted by future earthquakes to a significant extent.

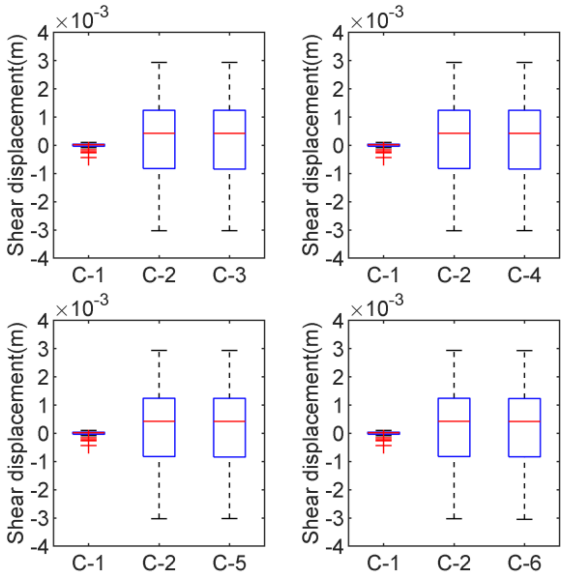

Figure 10. Effect of glacial and seismic loading on joint shear displacement (C-1: Case 1, C-2: Case 2, C-3: Case 3, C-4: Case 4, C-5: Case 5, C-6: Case 6)

5 CONCLUSIONS

This work aimed to quantify the effect of probable earthquakes on the conceptual DGR stability by performing a statistical analysis. Previous studies evaluated earthquake effects on the repository and showed a measured change in excavation damage zone due to low probability earthquake events. This study performed a quantitative analysis on a 2D model developed in the RS2 finite element package. The model was validated by comparing it to a previously reported repository seismic modeling. The model used a Voronoi network around the repository placement room to represent a crystalline host rock and was able to simulate geological perturbations such as glacial loading and earthquakes. The statistical method, analysis of variance, analyzed normal and shear stresses and displacements after earthquake events relative to the model with no earthquake events and no glacial loading. This study showed that, glacial loading caused additional damage in the repository excavation damage zone and had statistically significant effects on the joint normal stress. The seismic coefficients had no statistically significant effect on the joint parameters, although only the final state after the earthquake loading was investigated. Future research will examine the dynamic loading during an earthquake.

6 REFERENCES

Baeckblom, G., and Munier, R. 2002. Effects of earthquakes on the deep repository for spent fuel in Sweden based on case studies and preliminary model results. Swedish Nuclear Fuel and Waste Management Co.

Boyle, C.H., and Meguid, S.A. 2015. Mechanical performance of integrally bonded copper coatings for the long term disposal of used nuclear fuel. *Nuclear Engineering and Design*, 293: 403–412.

CNSC. 2018. Guidance on Deep Geological Repository Site Characterization.

Fisher, R.A. 1922. On the Interpretation of χ 2 from Contingency Tables, and the Calculation of P.

Fisher, R.A. 1954. Statistical Methods for Research Workers. *Oliver and Boyd*.

Guzina, Z.R.-, Riahi, A., and Damjanac, B. 2015. Long-Term Stability Analysis of APM Conceptual Repository Design in Sedimentary and Crystalline Rock Settings. *NWMO-TR-2015-27*, Itasca Consultant Group, Inc.

Hayes, G.P., Smoczyk, G.M., Villaseñor, A.H., Furlong, K.P., and Benz, H.M. 2020. Seismicity of the Earth 1900–2018. *In Scientific Investigations Map*. U.S. Geological Survey.

Kaláb, Z., Šílený, J., and Lednická, M. 2017. Seismic stability of the survey areas of potential sites for the deep geological repository of the spent nuclear fuel. *Open Physics*, 15(1): 486–493.

McEvoy, F.M., Schofield, D.I., Shaw, R.P., and Norris, S. 2016. Tectonic and climatic considerations for deep geological disposal of radioactive waste: A UK perspective. *The Science of the Total Environment*, 571: 507–521.

Montgomery, D.C., and Runger, G.C. 2007. Wiley: Applied Statistics and Probability for Engineers, 6e.

Noronha, J. 2016. Deep geological repository conceptual design report crystalline / sedimentary rock environment. Nuclear Waste Management Organization, *APM-REP-00440-0015 R001*: 191.

NWMO. 2014. APM Conceptual Design and Cost Estimate Update. Underground Repository Design Criteria. *Technical Memorandum. Doc No: APM-DCRI-22100-0001 revision R00e.*

NWMO. 2015. Description of a deep geological repository and centre of expertise for Canada's used nuclear fuel. Nuclear Waste Management Organization.

NWMO. 2018. Programs around the world for managing used nuclear fuel. Nuclear Waste Management Organization.

NWMO. 2019. Deep geological repository . Nuclear Waste Management Organization.

Sinha, S., and Walton, G. 2018. Application of Micromechanical Modeling to Prediction of In-Situ Rock Behavior. American Rock Mechanics Association.